Energy-Harvesting System-in-Package (SiP) Micro-System[1]

Erick O. Torres, *Student Member, IEEE*[2], and Gabriel A. Rincón-Mora, *Senior Member, IEEE*[3]

Abstract: As micro-scale devices, such as wireless micro-sensors and non-invasive biomedical implants, continue to shrink and incorporate more functions, energy becomes scarce, thereby shortening operation life. Furthermore, the limited volume space available constrains the stored energy available in state-of-the-art micro-battery technologies, such as thin-film lithium ion (Li Ion). For long-lasting life, it is therefore necessary to replenish continuously the energy consumed by harnessing, storing, and delivering energy from the environment *in situ*, i.e., in the package, alongside the application electronics. Operation life would ultimately be independent from storage limitations. The proposed self-contained, system-in-package (SiP) solution is composed of three different energy-harvesting sources (light, vibrations, and thermal gradients) that sustain the system, while a charger stores the harnessed energy into an in-package Li Ion. Since substantially low power levels are expected, the sensor must minimize energy consumption and the system must therefore be power-moded into various operational modes to consume power only when necessary. Experimental measurements show how an electrostatic harvester sources nano-scale currents that can supply 1.18 µW from typical vibrations and, thus, recover the system consumption within 37.3 s.

Energy Requirements of Micro-Systems

In today's high-tech world, microelectronic portable devices such as biomedical, military, structural, and environmental wireless micro-sensors incorporate numerous functions and therefore impose increasingly stringent power requirements on the system, in spite of every effort to limit the amount of energy required per function. Unfortunately, because of the volume constraints of portable electronics, the available, stored energy is limited, resulting in short operation life (i.e., short lifetime or runtime). To prolong the life of the device, the system must be managed efficiently, minimizing all power losses and eliminating unnecessary or redundant battery-draining events. In addition to designing a highly efficient system, researchers also seek to increase the energy density in batteries, but even at the fundamental limits, the solution has low and finite lifetimes. A long-lasting energy supply, independent of the amount of energy initially stored, is attractive and increasingly demanded in applications like biomedical implantable devices and structural-embedded systems, which is why a self-renewable energy reservoir that can continually self-replenish the energy that is consumed finds a niche in a wide variety of portable applications.

But how can this replenishing energy be harnessed from the surrounding environment and stored *in situ*? State-of-the-art micro-electromechanical system (MEMS) generators and transducers can extract energy from vibrations, thermal gradients, and even light exposure (Roundy et al. 2004). The energy extracted can then be stored in chip-compatible, rechargeable batteries such as thin-film lithium ion (Li Ion) (Ehrlich 2002; Bates et al. 2000). However, this

extracted energy is generally small and unpredictable, in the form of short intermittent bursts. It is therefore important to develop the electronics necessary to transfer this energy into the rechargeable battery and deliver it to the system without itself requiring much power to operate.

The proposed system solution harvests and transfers energy from photovoltaic, thermoelectric, and other MEMS generators to a rechargeable thin-film Li Ion, resulting in a long-lasting, self-sustaining microelectronic system capable of self-replenishing its own energy drain. Since harvested energy manifests itself in irregular, random "bursts," a discontinuous, intermittent charger is required to interface the energy-sourcing devices with the energy-storage reservoirs (e.g. lithium-ion batteries). The charger must harness sporadic trickles of energy supplied by the surroundings, convert them into usable power, and use them to charge a Li-Ion battery. Energy that is typically lost in the environment is therefore added back to the system, thereby decreasing or even eliminating the need for battery replacement and/or external recharge cycles. The goal of this project is to design an intermittent micro-power Li-Ion charger and integrate it with chip-compatible energy harvesters, storage elements, and micro-sensor device into a single plastic chip-package, resulting in a long-lasting, self-sustainable system-in-package (SiP) micro-system solution.

Background

Present-day technologies can scavenge vibrational, thermal, and solar energy from the environment. For the proposed self-harnessing system, this energy must then be stored in capacitors, batteries, and other electrochemical reservoirs. However, transferring this energy from its source to the storage devices must not only cater to the reservoir but also itself incur insignificant power losses. What is more, for a system-in-package (SiP) solution, all of these components

must somehow conform to the constraints of a silicon chip-package, in other words, they must all live and coexist in the same chip.

Energy Harvesting

Energy harvesting is defined as the conversion of energy already present in the surrounding environment into usable electrical energy. When compared with the energy stored in common storage elements like batteries, the environment represents a relatively inexhaustible source of energy. Consequently, energy harvesting (i.e., scavenging) methods must be characterized by their power density, rather than energy density. Light, for instance, can be a significant source of energy, but it is highly dependant on the application and how much exposure the device is subjected to (e.g., indoors versus outdoors, with power densities between 10 μW/cm^2 to 15 mW/cm^2). Yet, in a micro-scale system, photovoltaic cells must conform to substantially small surface areas, which can be challenging. Thermal energy, on the other hand, is limited because the gradients across a chip are typically considerably low, less than 10 ºC, capable of only harvesting up to 15 μW/cm^3. Kinetic energy from vibrations is a moderate source, with power density levels ranging between 1 to 200 μW/cm^3, but again dependent on the application. A stationary outdoor sensor may therefore benefit from harnessing light energy but a navigational indoor sensor may better reap the advantages of systematic vibrations. Table 1 summarizes and compares each of the energy conversion methods.

Light Energy

Photovoltaic cells convert incident light into electrical energy (Kasap 2001; Raffaelle et al. 2000; Warneke et al. 2002). Each cell consists of a reverse-biased pn$^+$ junction, where light interfaces with the heavily doped and narrow n$^+$-region (Figure 1(a)). Photons generate electron-

hole pairs within the depletion region, which the built-in electric field of the junction immediately separates so that electrons drift to the n^+-side and holes to the p-side. Positive and negative charges accumulate developing an open-circuit voltage. With a connected load across the cell, excess electrons travel through it from the n^+-side to recombine with holes at the p-side, generating a photocurrent that is directly proportional to light intensity and independent of cell voltage.

A current source with appropriate parasitic elements models the photovoltaic cell, as illustrated in Figure 1(b). A shunt parasitic diode represents the pn-junction, where the load voltage determines the forward-bias diode current. The total current delivered to the load is the difference between the generated photocurrent and shunting diode current. The surface distance traveled by each generated carrier (to reach the electrode) introduces series resistance, which is why, to minimize it, one of the electrodes completely covers the dark side and numerous thin finger electrodes permeate the illuminated side without significantly impeding light flow. Similarly, a shunt resistance represents photo-generated carriers that flow through the edges and surface of the cell rather than the load.

Typically, micro-systems employ thin-film photovoltaic cells. Because of size constraints, a single cell cannot provide significant power and, consequently, several cells are connected in parallel arrays to increase current. Research demonstrates that thin-film photovoltaic cells can provide sufficient power to a micro-system, although at lower efficiencies than their macro-scale counterparts (10-20 %) (Raffaelle et al. 2000; Warneke et al. 2002). Nevertheless, photovoltaic energy conversion offers higher output power levels, relative to other energy conversion mechanisms, in addition of being a mature technology compatible with mainstream integrated circuits (IC). Yet, its power output is heavily dependent on environmental conditions, and changes drastically with various light intensities.

Thermal Energy

Thermal gradients in the environment are directly converted to electrical energy through the Seebeck (thermoelectric) effect (Castano et al. 1997; DiSalvo 1999; Fleurial et al. 1999; Jacquot et al. 2004; Rowe 1999; Stordeur and Stark 1997; Wang et al. 2005). Temperature differentials between opposite segments of a conducting material result in heat flow and, consequently, charge flow, since mobile, high-energy carriers diffuse from high to low concentration regions. As carriers diffuse, a concentration gradient produces an electric field across the material that opposes the net diffusion of carriers, eventually forcing equilibrium conditions. At equilibrium, the carriers traveling back to the high temperature junction due to the electric field cancel the net number of hot carriers traveling towards the cold junction, and therefore, no voltage is established.

A thermocouple configuration, shown in Figure 2(a), is a more suitable approach for power generation by electrically joining n- and p-type materials at the hot end. Heat flow carries the dominant charge carriers of each material (electrons in n-type and holes in p-type) to the low temperature junction, respectively ionizing each base electrode with an opposite charge and therefore establishing a voltage differential across the low temperature base electrodes. As charge carriers depart the hot end, they leave behind ionized molecules that, instead of attracting the opposite flow of charge from the material itself, attract carriers from the opposite type material through a metallic, low impedance short. In the end, the generated voltage, modeled in Figure 2(b), and power are proportional to the temperature difference and the Seebeck coefficient of the material.

Large thermal gradients and proper material selection are essential to produce practical voltage and power levels. Nevertheless, temperature differences greater than 10 ºC are rare in a

micro-system (Roundy et al. 2004) that when coupled with the Seebeck coefficients of typical thermoelectric materials (100-200 µV/K) (Jacquot et al. 2004; Wang et al. 2005) lead to very low voltages per thermocouple. Placing several thermocouple elements in a series configuration (up to 2000) alleviates the necessity of large thermal gradients, but at the expense of very large series electrical resistance, which increases Ohmic power losses and adversely affects the overall power efficiency. As a result, low voltage levels are expected.

Vibration Energy

Energy extraction from vibrations is based on the movement of a "spring-mounted" mass relative to its support frame (mass-spring-damper system) (Roundy et al. 2003). Mechanical acceleration produced by vibrations cause the mass to move and oscillate. This relative displacement causes opposing frictional and damping forces to be exerted against the mass that absorb the kinetic energy of the initial vibration, thereby reducing and even extinguishing the oscillations. Intentionally imposing an electrical damping force with a magnetic field (electromagnetic), an electric field (electrostatic), or strain on a piezoelectric material harnesses the mechanical energy and converts it into electrical energy, and as a result, harvests energy from the surrounding environment.

Electromagnetic and piezoelectric energy harvesters use magnetic fields and piezoelectric materials, respectively, to convert mechanical energy to electrical. Electromagnetic harvesting exploits Faraday's law, where a voltage on a coil is produced as it oscillates across a magnetic field (or vice versa) (Amirtharajah and Chandrakasan 1998; Beeby et al. 2007; El-Hami et al. 2001; Kulah and Najafi 2004; Williams et al. 2001; Williams and Yates 1996). On the other hand, strain, or deformation, of a piezoelectric material causes charge separation across the device, producing a voltage drop proportional to the stress applied (Ottman et al. 2003; Roundy et

al. 2003; Roundy and Wright 2004; Sodano et al. 2004a,b). Both harvesting methods generate irregular time-varying ac voltages that, as a result, require additional circuitry to rectify and condition the extracted power. Power conditioning incurs additional power losses, and thus, affects adversely the overall power efficiency of the mechanisms. What is more, electromagnetic harvesters generate very low voltages (100-300 mV) that present further design challenges (Beeby et al. 2007). Still, both methods require exotic materials (magnetic and piezoelectric), which do not conform easily to micro-scale integration.

Electrostatic (capacitive) energy harvesting schemes rely on the work done against the electrostatic force of a vibration-dependant variable capacitor (or varactor) (Meninger et al. 2001; Roundy et al. 2002; Roundy et al. 2003; Stark et al. 2006; Torres and Rincón-Mora 2006). As vibrations cause the capacitance of the varactor to decrease, under constant charge or voltage conditions, mechanical energy is converted to electrical. When constraining charge, the capacitor is open-circuited, confining the initial charge in the capacitor and therefore forcing the voltage to change accordingly ($Q_{Constant} = C_{VAR}V$) and, as a result, the potential energy in the capacitor increases ($E_{CAP} = \frac{1}{2}C_{VAR}V^2$). Unfortunately, the maximum capacitor voltage increases beyond the rated breakdown limits of typical semiconductor technologies, limiting its implementation to less popular and often more expensive processes (Stark et al. 2006). Perhaps a more practical and benign approach is to hold the voltage across the variable capacitor constant, where as vibrations force capacitance C_{VAR} to decrease, charge Q is driven out of the device ($Q = C_{VAR}V_{Constant}$) and into a battery, an energy reservoir with pre-defined voltage levels (Torres and Rincón-Mora 2006). For instance, as shown in Figure 3, a diode connects the battery to the varactor and clamps the capacitor to battery voltage V_{BAT}, producing harvesting current i_{HARV} that directly charges the battery.

Energy Storage

Fundamentally, energy harvesters are low power sources with a virtually unlimited energy supply, but their intermittent nature limits their use. Even if the system is designed to operate under low average power conditions, energy-harvesting sources can be ineffective and impractical because energy is not supplied continuously, but rather in intermittent and spontaneous spurts, and therefore not necessarily available when required. Moreover, micro-sensors must accommodate several high instantaneous power functions, such as data transmission, that energy-harvesting sources simply cannot supply. A more practical approach is to store, when possible, converted energy in energy-storage elements capable of supplying power and energy on-demand, when needed. Typical energy-storage devices in a micro-system include capacitors, inductors, and batteries.

Passive storage elements, such as capacitors and inductors, store electrical energy in either electric or magnetic fields, respectively. Capacitors, for instance, can supply instantaneous current, but only sustain it for a short time because of low energy storage capabilities at micro scales. Inductors integrated in a micro-system, on the other hand, feature small inductance values and develop weak magnetic fields because of few turns, low currents, and lack of strong magnetic core. Notwithstanding, capacitors and inductors are useful as intermediate, short-term energy storage devices, especially when transferring energy from its original source to a more capable energy-storage device, such as a battery.

Batteries store electrical energy chemically. Energy is released as electricity through a chemical reaction inside the battery cell that transfers electrons from its anode to its cathode across an electrolyte material (Linden 2002). Recharging the battery reverses this reaction and stores electrical energy back in the form of chemical bonds. Conventional chemistries, such as

nickel zinc (NiZn), nickel-metal hydride (NiMH), and nickel cadmium (NiCd), offer high energy densities and good discharge rates, but also feature short cycle life and adverse "memory" effects. Lithium-ion batteries (Li Ion) overcome these drawbacks, with higher energy density and discharge rate, higher cell voltage, longer cycle life, and nonexistent "memory" effects. Thin-film technology (less than 15 μm thickness) promises to permit the integration of lithium-ion batteries into a micro-system while capable of delivering relatively high power levels (Bates et al. 2000). A disadvantage is their sensitivity to overcharge and over-discharge. If the cell voltage increases above 4.2 V, or decreases below 2.7 V, the battery will significantly degrade, and in some cases, even vent and explode. Careful energy management during the charging and discharging processes is essential to maximally extend battery life and usable capacity.

Charging Circuitry

The charger is the interface between the energy harvester and the battery, transferring energy from source to storage. Maximum battery life, capacity, and energy content require a power-efficient charger design. A constant-current/constant-voltage charging scheme, illustrated in Figure 4, achieves such purpose for lithium-ion batteries. The initial phase preconditions the battery with a low charging current, ensuring the cell is ready (voltage is at least 2.7 V) for a full charge cycle, which terminates at the end-of-charge voltage, typically around 4.2 V. When ready, a constant current charges the battery. The charging current cannot exceed 1.5 C to avoid premature aging, electrolyte disassociation, and other damages to the cell, where C is the nominal capacity or ampere-hour rating of the battery and refers to the discharge current required to exhaust the energy in the battery in one hour. For instance, a 10 mAh battery cell (i.e., 10 mAh is 1 C, in other words, a 10 mA load for 1 hour completely discharges the battery) should not be charged with a current beyond 15 mA (1.5 C) to avoid damages. When the voltage nears the end-of-

charge threshold (4.2 V), a constant voltage is applied to the battery, effectively supplying a slowly decreasing charging current, until an end-of-charge current value is reached (typically around $C/10$), at which point the whole charge cycle is completed. For a fast charge cycle, the constant-voltage phase may be skipped, but at the cost of usable capacity (only 40% to 70% of usable capacity is achieved) (Lopez et al. 2004). As a result, both charging steps are required to charge the battery completely.

The charging circuit depends on the nature of the input energy that is to be stored in the battery. Mainly, the charging current applied to the battery can be either continuous or discontinuous. Continuous charging techniques may utilize linear and switching regulators. A linear regulator linearly controls the conductance of a series pass device via a feedback loop to regulate the output against variations in load current and supply voltage, continuously supplying current (Chen and Rincón-Mora 2006). Linear regulators are analogous to resistive voltage dividers in that they can only source voltages below the input supply. Switching regulators, on the other hand, can boost (step-up) or buck (step-down) the input voltage (Formenti and Martinez 2004). In this latter scheme, fully on or off switching devices alternately store and deliver energy, as regulated by a feedback loop, to the load via a combination of inductors and capacitors. The switching nature of these regulators inherently achieves high power efficiency because the switches incur negligible voltage drops, even at high current levels, thereby dissipating little power, when compared to the series pass device of the linear regulator. Although the circuit switches, the output is regulated and can continuously supply a charge current, albeit with a noisy ac ripple.

Discontinuous charging refers to the application of alternating and discrete charge current pulses to the battery. The duty cycle of the pulsating current waveform gradually decreases as

full charge conditions are approached. Efficiency is improved because periodically interrupting the charge current allows ions to diffuse and redistribute more evenly, thereby reaching higher capacity levels (Cope and Podrazhansky 1999). Adding a brief discharge pulse after each charging pulse further accelerates this diffusion process. This charging scheme is most compatible with intermittent and irregular sources, such as vibration-based electrostatic harvesters.

Voltage and current feedback control loops not only protect the battery cell from overcharge and over-discharge but also regulate the charging process. The transition between charging steps, which is controlled by the feedback loops, is vital for an efficient and safe charging process (Chen and Rincón-Mora 2006). A diode is used to determine which feedback loop dominates and dictates the charging phase. During the constant-current phase, the current feedback loop dominates, regulating the charging current. The current feedback control loop can also perform the preconditioning phase and the end-of-charge current and over-current detection by sensing the current through a series sense resistor (Lima et al. 2003). As the cell voltage nears the end-of-charge voltage (e.g., 4.2 V), the voltage feedback loop begins to acquire control from the current loop, regulating the cell voltage and supplying the necessary current to maintain the voltage constant, which decreases as the battery reaches full capacity.

Energy Harvesting System-in-Package (SiP) Micro-Sensor

To overcome the inadequate energy availability featured by state-of-the-art micro-scale storage devices, the proposed micro-sensor intends to harvest ambient energy in the form of light, vibrations, and thermal gradients to power its functions, including sensing and telemetry. Each harvester features very low power levels and, consequently, the system requires very efficient power management and load multiplexing. What is more, to maintain the non-invasive and economical nature of micro-sensing applications, a single package encompasses all system com-

ponents, including harvesters. The micro-system, as a result, continuously restocks its consumption *in situ* and thereby is able to extend its operational lifetime indefinitely.

Integration

The proposed system fully integrates into a single plastic package three different ambient energy sources with storage devices, a sensor load, and the circuitry necessary to power and operate the sensor, resulting in a self-contained, self-sustaining system-in-package (SiP) micro-sensor (Figure 5). A thin-film lithium-ion micro-battery stores the energy from vibrations, light, and thermal gradients by way of an efficient charger and delivers it to its sensor load through a voltage regulator circuit, as Figure 6 illustrates.

The photovoltaic panel is exposed to light and its harvested energy is delivered to the battery via bondwires and the charger circuit. Part of the solar energy is lost as heat, which raises the temperature of the panel and establishes a high temperature on top of the thermopiles. The cold junction of the thermoelectric layer is connected to the printed circuit board (PCB) ground via a thermally conductive path, acting as a heat sink (i.e., thermal ground). The resulting thermal gradient across the thermoelectric generator produces a harvesting voltage (Whitacre et al. 2002), which is used to also charge the battery. The photovoltaic layer serves two functions, as a result, improving its operational efficiency. Additionally, a MEMS variable capacitor (i.e., a varactor) harvests energy from vibrations through electrostatic means. As the capacitance of the varactor changes with vibrations, movement and acceleration are sensed. Motion can therefore be extracted from corresponding changes in capacitance, and energy scavenged is thusly its metric. As a result, the MEMS capacitor functions as both a motion sensor and an energy harvester, again maximizing the functional efficiency of the system. Each harvesting source collaborates

13

and complements each other to provide sufficient energy for the system to operate. In the end, energy harvested from the surrounding environment continually powers the SiP system.

The electrostatic MEMS-based harvester is compatible with mainstream IC technologies, which is its most attractive feature. MEMS varactors are typically fabricated through relatively mature silicon micromachining techniques, such as deep reactive ion etching (DRIE) (Roundy et al. 2003). The movement of the capacitor plate is preferably in-plane (in parallel) with the substrate to avoid problems associated with out-of-plane capacitors, such as large mechanical damping and surface interactions. The capacitor plates for in-plane motions are typically fabricated with inter-digitated fingers in a comb structure, where varying overlap area, as shown in Figure 7(a), provides greater plate displacements and can achieve very low minimum capacitances (~ 0.1 pF), but suffer from stability problems. Changing gap distance, illustrated in Figure 7(b), on the other hand, provides a more stable solution due to smaller spring deflections with large maximum capacitances (~ 800 pF) but at the expense of greater minimum capacitances (~ 20 pF) (Roundy et al. 2003). Regardless of the mechanical design, parasitic capacitors develop between the moving plate and the substrate and sidewalls, which require more initial charge and energy, while the capacitor plates will create parasitic series resistance. The complete electrical model of the variable capacitor is illustrated in Figure 7(c).

Other system components, such as the thin-film lithium-ion micro-battery and supplementary circuitry, occupy separate substrates. The microelectronic circuit layer houses the control circuits of the energy sources, micro-sensor interface electronics, and battery charger, plus all other safety functions. Each substrate is interconnected with one another through the package's leadframe and respective wirebonds, all inside a single plastic package, as conceptually illustrated in Figure 5.

Energy Management and System Load

Since all energy sources depend on the conditions of the surrounding environment, extracted energy is intermittent and random in nature, not continuous. Therefore, the proposed system requires a charger that is compatible with such irregular, intermittent energy sources. The charger must therefore be smart enough to accumulate enough energy before transferring it to the battery. A specially designed transitional capacitor is a viable candidate for this purpose. The charger must then combine all three intermittent energy sources and store the collective energy into a single energy storage device, the lithium-ion battery, in this case, as shown in Figure 6. The battery then delivers energy to the sensor load through a regulator circuit.

At any given time, the amount of available energy is low, given the low power output of each harvesting source. Consequently, the sensor load must consume minimal power and a time-division multiplex approach is therefore employed. The system functions are divided into different operational modes assigned to consume power in finite bursts, only when needed. Each operational mode, such as data acquisition and processing, transmission, and reception, is allocated asynchronous, low duty-cycle time-segments during which the battery provides the necessary power (Figure 8). Throughout the rest of the cycle, the energy harvesters recover consumed energy and restore it into the battery.

Typically, sensing functions are supplied about 10 μW of power for 1 s, while 5 mW for 10 ms are dedicated to wireless transmission and reception (telemetry functions) (Harb et al. 2002). In the proposed system, 5 mW for 5 ms are allocated for transmission and 3.75 mW for another 5 ms for data reception. Motion sensing and energy harvested from vibrations are correlated, which is why battery voltage is used as the metric of motion and sensed after each recovery period. Voltage monitoring, an already essential component of the charger, serves a dual

function. A simple low power and slow analog-to-digital converter (ADC) senses this battery voltage and converts it to a digital word for transmission. This sensing task is estimated to last about 1 ms, less than previously estimated, and consume less than 10 µW. The combined energy output of the harvesters, statistically speaking, fully supplies the system just described, allowing it to function continually without external charging cycles or battery swaps.

It is important that all high power tasks are executed when enough energy is stored in the battery. Assuming at least an average harvested power of 100 µW throughout the entire cycle, the system can recover its energy consumption in at least 440 ms, as summarized in Table 2. Harvesting functions are continually performed, and only sensor and telemetry tasks are given specific time assignments. For more random conditions, the system will enter an asynchronous mode, whereby transmission only occurs if enough energy is stored, in other words, if enough sensing activity is detected, which implies the energy harvested sets both the frequency and duty cycle of the system.

Experimental Harvesting Results

The proposed system harvests kinetic energy from vibrations as the capacitance of a voltage-constrained varactor decreases. Vibrations work against the electrostatic force of the capacitor, energizing charges to flow, and as a result, develops a harvesting current that charges an energy storage device, that is, a thin-film Li Ion. The specific embodiment of the harvesting circuit features a pre-charged varactor (at maximum capacitance) connected to the battery through a diode (Figure 3). As its capacitance decreases, the diode clamps the varactor voltage to the battery and allows the resultant harvesting current to charge the battery directly.

To test the viability of the harvesting scheme, a trimmer variable capacitor, which is manually pre-charged and turned, emulates the harvesting device under vibration conditions. A 3

V supply emulates a moderately charged Li Ion (V_{BAT}), whose full range normally spans 2.7 to 4.2 V. Electrolytic and ceramic capacitors connected from V_{BAT} to ground filter away any noise from the supply. After setting the trimmer capacitor to its maximum capacitance, it is manually pre-charged by momentarily short-circuiting it to V_{BAT}. The trimmer capacitor features a measured maximum-minimum capacitance range of approximately 250 to 60 pF, including parasitic capacitances.

As the capacitor is turned and its voltage is constrained by the diode, the resulting harvesting current is recorded. This current is on the order of nano-amperes and measuring it presents a challenge. To this end, a high-accuracy resistor (±1%) in series with the diode senses the harvesting current, which according to Ohm's law, generates a sense voltage that is the product of its current and resistance, as the schematic in Figure 9 shows. Still, the resulting sense voltages are substantially small, even with large resistance values, and therefore require amplification with a high-precision instrumentation amplifier. The amplifier must be accurate and high bandwidth (to detect rapidly changing currents accurately), yield high gain, reject common-mode noise, introduce little noise, and have low input-referred offsets to avoid compromising the validity of the measurement. Two amplifiers in series achieve the gain necessary, but still, any offset, noise, and/or unwanted signal present near the inputs is also amplified, resulting in a noise-sensitive circuit. Noise can be filtered by introducing a substantially low-frequency pole in one of the amplifiers and effectively converting it into a low-pass filter, but this sacrifices bandwidth and the ability to accurately detect the rapidly changing current. A better solution is to filter noise at the amplifier input by placing a parallel capacitance with the sense resistor, which diverts high frequency noise power away from the sensing resistor. Thermal noise in the resistor is not a significant factor because of the low currents involved. To further protect the circuit from

external noise, the circuit board is operated from inside a grounded Faraday box that protects it from electromagnetic noise (from cell phones, light bulbs, power cables, etc.) normally present in the environment. Finally, the accuracy of the sensing circuit was calibrated with a separate current source and the sensing resistance was measured to offset any inaccuracies resulting from input-voltage offsets, gain variations, and resistance variations.

Figure 10(a) shows the harvesting current driven through the diode to the battery supply as the trimmer capacitor turns. During harvesting, capacitor voltage V_{C-VAR} is higher than V_{BAT} (about 3.5 V) because of the diode voltage drop that exists during current conduction. Turning the capacitor is a manual process and the device's response is consequently nonlinear, as the results show. Integrating the power harvested, which is the product of the measured current and battery voltage V_{BAT}, over the cycle time for 8 separate measurements yielded an average of 5.82 nJ per cycle. For the test measurement in Figure 10(a), a total of 6.37 nJ was harvested in a single cycle, as Figure 10(b) shows.

For the harvesting process to commence, an initial energy investment from the battery is required, which in this case is about 1.13 nJ per cycle, assuming an ideal lossless circuit pre-charges the capacitor. As a result, the battery stores a net energy gain of 4.72 nJ per cycle, on average. Typical environments feature peak vibration accelerations near 250 Hz (Roundy et al. 2003), or 4 ms per cycle, which would result in an average power gain of 1.18 μW. By only considering the electrostatic harvester with the estimated power loads of telemetry and sensing functions previously discussed, the system can recover its energy consumption in at least 37.3 s, as summarized in Table 3.

Discussion

18

The previous results showed that electrostatic energy harvesting is possible and measurable. Yet, many technical challenges remain. For instance, a pre-charger circuit must transfer the necessary energy investment to the variable capacitor as efficiently as possible, while also synchronizing and adapting to different and varying sources of vibration (Torres and Rincón-Mora 2006). Another challenge is to measure experimentally the harvesting current unobtrusively, without a series resistance, where one possibility is to replicate the harvesting current with a current mirror.

The system requires maximum efficiency, as it operates under low energy and power conditions. Collaboration between system components becomes necessary to reduce work and energy requirements. The operational efficiency of the photovoltaic panel, voltage monitor, and MEMS variable capacitor exemplify the effective cooperation and functional efficiency desired in the system. With minimal losses, ambient energy suffices to cater to the needs of the system. As a result, the system operates autonomously, without any direct external involvement. What is more, all system components are integrated into a single device, resulting in a long-lasting, self-sufficient system-in-package (SiP) micro-sensor solution.

Conclusion

The proposed self-powered, self-sustaining system-in-package (SiP) solution harnesses, stores, and delivers energy from the surrounding environment to the loading sensor application *in situ*, serving as a virtually endless source of energy. The life of the system is independent of the energy initially stored, as the system replenishes its own consumption by harvesting and transferring energy from three different harvesting sources into a micro-battery; experimental measurement results show how a variable capacitor harvests such a charging current. In the proposed approach, the battery not only supplies power to the charger and regulator circuits but also to the

sensor load. Light, thermal gradients, and mechanical vibrations supply the necessary energy to fully sustain the system. This harvested energy manifests itself in the form of small, intermittent "bursts," which is why an intermittent boosting charger is required. Since the power harvested is still in the micro-watt scale, the functions of the system are subjected to a time-division multiplex scheme, whereby functions are allocated power and time slices, and only operate when enough energy exists. The system, in the end, constantly restores the energy consumed after every drain event, and does not require replacement of exhausted and/or depleted supplies and/or batteries. This is an attractive feature for portable electronics and applications with limited accessibility, such as structural-embedded and biomedical implantable devices, just to name a couple.

References

Amirtharajah, R. and Chandrakasan, A.P. (1998). "Self-powered signal processing using vibration-based power generation." *IEEE Journal of Solid-State Circuits*, 33(5), 687-695.

Bates, J.B., Dudney, N.J., Neudecker, B., Ueda, A., and Evans, C.D. (2000). "Thin-film lithium and lithium-ion batteries." *Solid State Ionics*, 135(1-4), 33-45.

Beeby, S.P., Torah, R.N., Tudor, M.J., Glynne-Jones, P., O'Donnell, T., Saha, C.R., and Roy, S. (2007). "A micro electromagnetic generator for vibration energy harvesting." *Journal of Micromechanics and Microengineering*, 17(7), 1257-1265.

Castano, E., Revuelto, E., Martin, M.C., Garcia-Alonso, A., and Gracia, F.J. (1997). "Metallic thin-film thermocouple for thermoelectric microgenerator." *Sensors and Actuators A*, 60(1-3), 65-67.

Chen, M. and Rincón-Mora, G.A. (2006). "Accurate, compact, and power-efficient Li-Ion battery charger circuit." *IEEE Transactions on Circuits and Systems*, 53(11), 1180-1184.

Cope, R.C. and Podrazhansky, Y. (1999). "The art of battery charging." *Proc., 14th Annual Battery Conference on Applications and Advances*, IEEE, Piscataway, NJ, USA, 233-235.

DiSalvo, F.J. (1999). "Thermoelectric cooling and power generation." *Science*, 285(5428), 703-706.

Ehrlich, G.M. (2002). "Lithium-ion batteries." *Handbook of Batteries*, B. Linden and T.B. Reddy, eds., McGraw-Hill, New York, NY, USA, 35.1-94.

El-Hami, M., Glynne-Jones, P., White, N.M., Hill, M., Beeby, S., James, E., Brown, A.D., and Ross, J.N. (2001). "Design and fabrication of a new vibration-based electromechanical power generator." *Sensors and Actuators A*, 92(1-3), 335-342.

Fleurial, J.P., Snyder, G.J., Herman, J.A., Giauque, P.H., Phillips, W.M., Ryan, M.A., Shakkottai, P., Kolawa, E.A., and Nicolet, M.A. (1999). "Thick-film thermoelectric microdevices." *Proc., 18th International Conference on Thermoelectrics*, IEEE, Piscataway, NJ, USA, 294-300.

Formenti, J., and Martinez, R. (2004). "Design trade-offs for switch-mode battery chargers." *Portable Power Design Seminar*, Texas Instruments, Dallas, TX, USA, 4.1-4.16.

Harb, J.N., LaFollette, R.M., Selfridge, R.H., and Howell, L.L. (2002). "Microbatteries for self-sustained hybrid micropower supplies." *Journal of Power Sources*, 104(1), 46-51.

Jacquot, A., Chen, G., Scherrer, H., Dauscher, A., and Lenoir, B. (2004). "Modeling of on-membrane thermoelectric power supplies." *Sensors and Actuators A*, 116(3), 501-508.

Kasap, S.O. (2001). "Photovoltaic Devices." *Optoelectronics and Photonics: Principles and Practices*, Prentice-Hall, Upper Saddle River, NJ, USA, 254-272.

Kulah, H. and Najafi, K. (2004). "An electromagnetic micro power generator for low-frequency environmental vibrations." *Proc., 17th International Conference on Micro Electro Mechanical Systems (MEMS)*, IEEE, Piscataway, NJ, USA, 237-240.

Lima, F., Ramalho, J.N., Tavares, D., Duarte, J., Albuquerque, C., Marques, T., Geraldes, A., Casimiro, A.P., Renkema, G., Been, J., and Groeneveld, W. (2003). "A novel universal battery charger for NiCd, NiMH, Li-ion, and Li-polymer." *Proc., 29th European Solid-State Circuits Conference*, IEEE, Piscataway, NJ, USA, 209-212.

Linden, D. (2002). "Basic concepts." *Handbook of Batteries*, B. Linden and T.B. Reddy, eds., McGraw-Hill, New York, NY, USA, 1.3-18.

Lopez, J., Gonzalez, M., Viera, J.C., and Blanco, C. (2004). "Fast-charge in lithium-ion batteries for portable applications." *Proc., 26th Annual International Telecommunications Energy Conference*, IEEE, Piscataway, NJ, USA, 19-24.

Meninger, S., Mur-Miranda, J.O., Amirtharajah, R., Chandrakasan, A.P., and Lang, J.H. (2001). "Vibration-to-electric energy conversion." *IEEE Transactions on Very Large Scale Integration (VLSI) Systems*, 9(1), 64-76.

Ottman, G.K., Hofmann, H.F., and Lesieutre, G.A. (2003). "Optimized piezoelectric energy harvesting circuit using step-down converter in discontinuous conduction mode." *IEEE Transactions on Power Electronics*, 18(2), 696-703.

Raffaelle, R.P., Underwood, J., Scheiman, D., Cowen, J., Jenkins, P., Hepp, A.F., Harris, J., and Wilt, D.M. (2000). "Integrated solar power systems." *Proc., 28th Photovoltaic Specialists Conference*, IEEE, Piscataway, NJ, USA, 1370-1373.

Roundy, S., Steingart, D., Frechette, L., Wright, P., and Rabaey, J. (2004). "Power sources for wireless sensor networks." *Proc., 1st European Wireless Sensor Networks Workshop*, Springer-Verlag, Berlin, Germany, 1-17.

Roundy, S. and Wright, P.K. (2004). "A piezoelectric vibration based generator for wireless electronics." *Smart Materials and Structures*, 13(5), 1131-1142.

Roundy, S., Wright, P.K., and Pister, K.S. (2002). "Microelectrostatic vibration-to-electricity converters." *Proc., International Mechanical Engineering Congress and Expo*, ASME, New York, NY, USA, 487-496.

Roundy, S., Wright, P.K., and Rabaey, J. (2003). "A study of low level vibrations as a power source for wireless sensor nodes." *Computer Communications*, 26(11), 1131-1144.

Rowe, D.M. (1999). "Thermoelectrics, an environmentally friendly source of electrical power." *Renewable Energy*, 16(1-4), 1251-1256.

Sodano, H.A., Inman, D.J., and Park, G. (2004a). "A review of power harvesting from vibration using piezoelectric materials." *The Shock and Vibration Digest*, 36(3), 197-205.

Sodano, H.A., Park, G., Inman, D.J. (2004b). "Estimation of electric charge output for piezoelectric energy harvesting." *Strain*, 40(2), 49-58.

Stark, B.H., Mitcheson, P.D., Miao, P., Green, T.C., Yeatman, E.M., and Holmes, A.S., (2006). "Converter circuit design, semiconductor device selection and analysis of parasitics for micropower electrostatic generators." *IEEE Transactions on Power Electronics*, 21(1), 27-37.

Stordeur, M. and Stark, I. (1997). "Low power thermoelectric generator – self-sufficient energy supply for micro systems." *Proc., 16th International Conference on Thermoelectrics*, IEEE, Piscataway, NJ, USA, 575-577.

Torres, E.O. and Rincón-Mora, G.A. (2006). "Electrostatic energy harvester and Li-Ion charger circuit for micro-scale applications." *Proc., Midwest Symposium on Circuits and Systems*, IEEE, Piscataway, NJ, USA, 65-69.

Wang, W., Jia, F., Huang, Q., and Zhang, J. (2005). "A new type of low power thermoelectric micro-generator fabricated by nanowire array thermoelectric material." *Microelectronic Engineering*, 77(3-4), 223-229.

Warneke, B.A., Scott, M.D., Leibowitz, B.S., Zhou, L., Bellew, C.L., Chediak, J.A., Kahn, J.M., Boser, B.E., and Pister, K.S. (2002). "An autonomous 16 mm^3 solar-powered node for distributed wireless sensor networks." *Proc., IEEE Sensors*, IEEE, Piscataway, NJ, USA, 2, 1510-1515.

Whitacre, J., Fleurial, J.P., Mojarradi, M., Johnson, T., Myung, N., Ryan, A., and Neigh, S. (2002). "An integrated power generation and storage system: the power tile." *Micropower and Microdevices: Proceedings of the International Symposium*, E.J. Brandon, A. Ryan, J. Harb, and R. Ulrich, eds., Electrochemical Society, Pennington, NJ, USA, 203-214.

Williams, C.B., Shearwood, Harradine, M.A., Mellow, P.H., Birsch, T.S., and Yates, R.B. (2001). "Development of an electromagnetic micro-generator." *IEE Proceedings – Circuits, Devices, and Systems*, 148(6), 337-342.

Williams, C.B. and Yates, R.B. (1996). "Analysis of a microelectric generator for microsystems." *Sensors and Actuators A*, 52(1-3), 8-11.

Tables

Table 1. Comparison between Different Energy Harvesting Methods

Energy Conversion Method	Advantages	Disadvantages	Challenge in Micro-system
Photovoltaic	• No moving parts, reliable • Mature technology • Scalable	• Highly dependant on surrounding light conditions	• Small surface areas
Thermoelectric	• No moving parts, reliable • Scalable • Durable	• Very low conversion efficiency • Low output voltage	• Low temperature gradients
Piezoelectric	• No voltage source required • Higher output power and voltage	• Rectification and power conditioning • Moving parts	• Difficult integration of piezoelectric material • Decreased coupling and brittleness of thin-films
Electrostatic	• Scalable • Compatible with current technology	• Energy investment requirement • Synchronization with vibrations • Moving parts • High voltages (charge-constrained)	• Mechanical stability
Electromagnetic	• No voltage source required	• Rectification and power conditioning • Very low output voltage • Moving parts	• Difficult integration of magnet

Table 2. Estimates of Sensor Energy Consumption and Energy-Harvesting Source Requirements

System Requirements				Energy-Harvesting Source Requirements	
System Tasks	**Duration**	**Power**	**Energy**	**Energy Source**	**Expected Average Power (within 1 cm^2)**
Transmission	5.00 ms	5.00 mW	25.00 µJ	**Electrostatic**	50.00 µW
Reception	5.00 ms	3.75 mW	18.75 µJ	**Photovoltaic**	50.00 µW
Sensing	1.00 ms	10.00 µW	10.00 nJ	**Thermoelectric**	15.00 µW
Total: (500 ms cycle)	500.00 ms	88.00 µW	~ 44.00 µJ	**Total Average Power Available**	115.00 µW
Harvesting Requirement	> 440.00 ms	100.00 µW	**44.00 µJ**	**Total Available Energy per Cycle (500 ms)**	**57.50 µJ**

Table 3. Load Duty Cycle Requirements Based on Experimental Harvesting Results

Load Duty Cycle Requirements			
System Tasks	Duration	Power	Energy
Transmission	5.00 ms	5.00 mW	25.00 μJ
Reception	5.00 ms	3.75 mW	18.75 μJ
Sensing	1.00 ms	10.00 μW	10.00 nJ
Harvester Requirement:	> 37.29 s	1.18 μW	44.00 μJ

Figure Captions

Figure 1.   (a) Photovoltaic cell and (b) its circuit model.

Figure 2.   (a) Thermoelectric energy converter composed of two series thermocouples and (b) its circuit model.

Figure 3.   Voltage-constrained electrostatic energy harvester with a diode clamping the capacitor voltage $V_{C\text{-}VAR}$ to battery voltage V_{BAT}.

Figure 4.   Constant-current/constant-voltage model.

Figure 5.   Physical profile view of the proposed system-in-package (SiP) micro-sensor.

Figure 6.   Electrical diagram of the proposed system-in-package (SiP) micro-sensor.

Figure 7.   (a) Changing overlap area and (b) gap distance in-plane variable capacitors, and (c) an energy harvesting circuit highlighting the model of the variable capacitor.

Figure 8.   Power profile of the system in a 500 ms cycle.

Figure 9.   Experimental test setup with series sense resistor R_{SENSE}, filtering capacitor C_{SENSE}, and two back-to-back 100 V/V instrumentation amplifiers.

Figure 10. Electrostatic harvester measurements showing (a) harvesting current i_{HARV} and (b) extrapolated energy profile E_{HARV}.

Figures

(a)   (b)

Figure 1

N-type Material
P-type Material
Metal Conductor (Al)
Thermal Conductor
Thermal Insulator (SiO_2)

Heat Flow

T_{hot}

j_n j_p

v_{TH1} v_{TH2}

Heat Sink

T_{cold}

$-$ v_{OC} $+$

(a)

R_s

$v_{Thermal}$ v_{OC}

$+$

$-$

$v_{Thermal} = v_{TH1} + v_{TH2}$

(b)
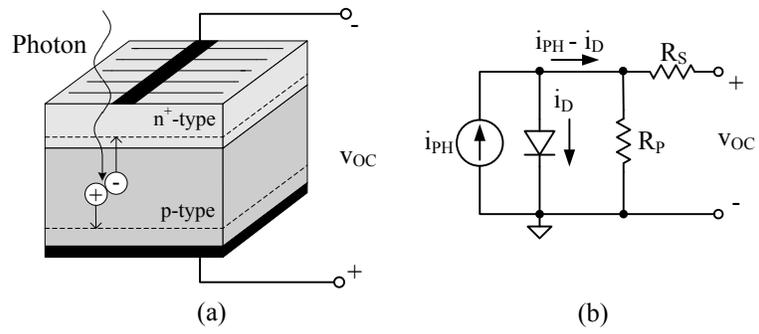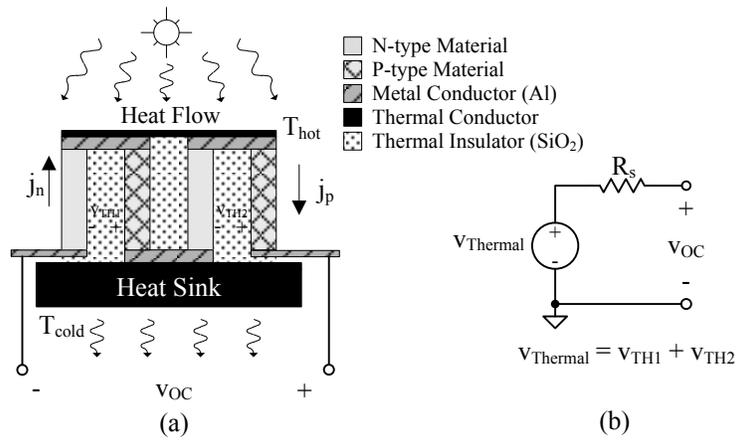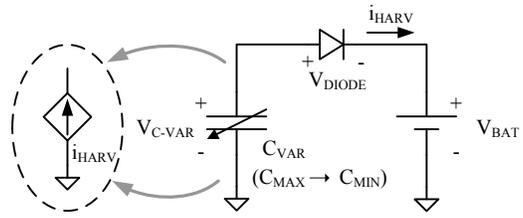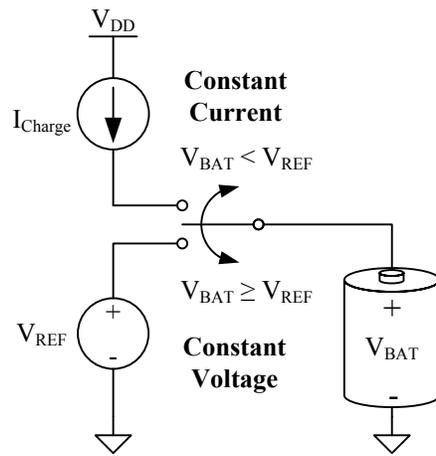
Figure 2

Figure 3

Figure 4
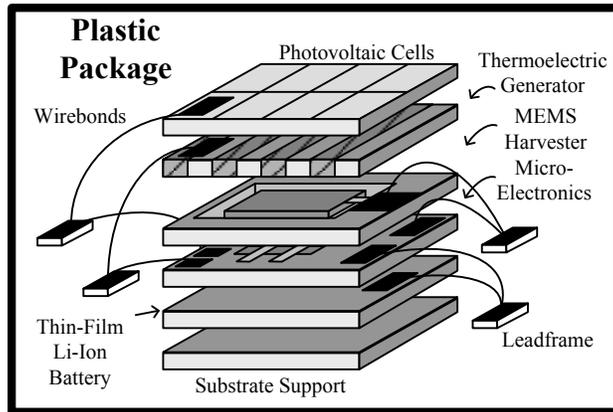
Figure 5

System-in-Package (SiP) Solution

Figure 6

(a)   (b)   (c)

Figure 7

Figure 8

G_1
100 V/V
G_2
100 V/V

$V_R = i_{HARV}R_{SENSE}$

$+ \quad V_R \quad -$

$+ \quad IA_1 \quad -$

$+ \quad IA_2 \quad -$

$V_{SENSE} = V_R G_1 G_2$

i_{HARV}

D

R_{SENSE}
10 kΩ

$+ \quad V_{DIODE} \quad -$
0.5 V

i_{HARV}

V_{SUPPLY}
3 V

$V_{C\text{-}VAR}$
3.5 V

$+$
$-$

C_{VAR}
250-60 pF
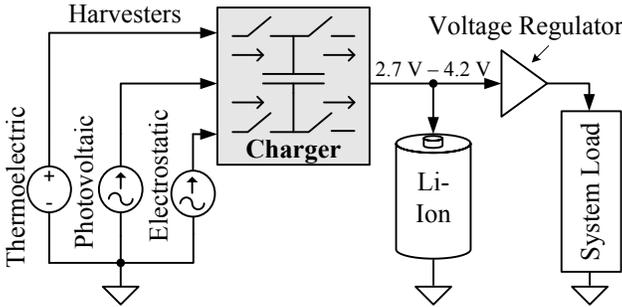
C_{SENSE}
10 nF
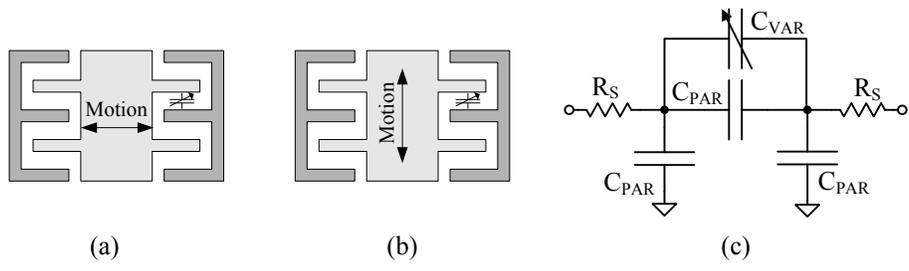
$C_{SUPPLY1}$
470 µF
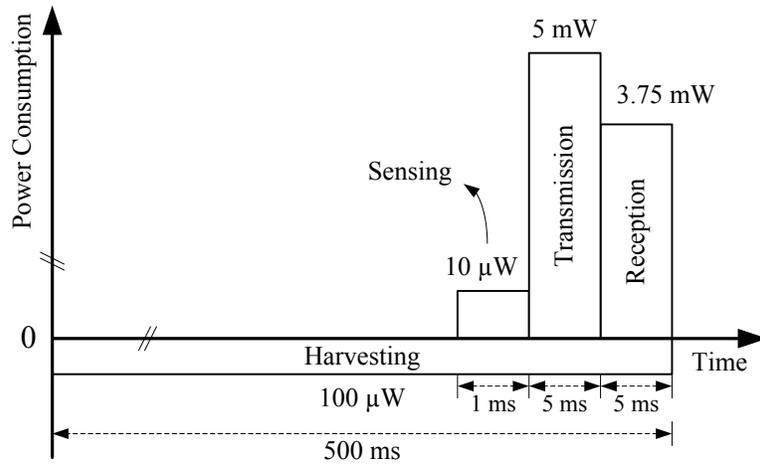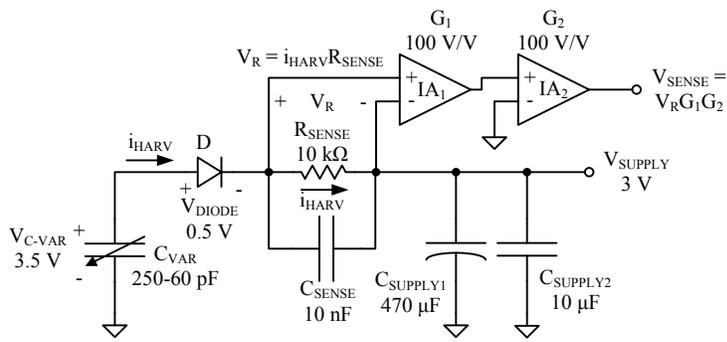
$C_{SUPPLY2}$
10 µF

Component	Note
R_{SENSE}	Thick Film ±1%
C_{SENSE}	Ceramic
$C_{SUPPLY1}$	Electrolityc
$C_{SUPPLY2}$	Ceramic
C_{VAR}	Sprague-Goodman GZC18100
$IA_{1,2}$	Linear Technology LTC1100
D	1.5 µm CMOS IC

Figure 9

(a)

(b)

Figure 10